Human Protein Complex-Based Drug Signatures for Personalized Cancer Medicine

Fei Wang, Yulian Ding, Xiujuan Lei, *Member, IEEE*, Bo Liao, and Fang-Xiang Wu, *Senior Member, IEEE*

***Abstract*—Disease signature-based drug repositioning approaches typically first identify a disease signature from gene expression profiles of disease samples to represent a particular disease. Then such a disease signature is connected with the drug-induced gene expression profiles to find potential drugs for the particular disease. In order to obtain reliable disease signatures, the size of disease samples should be large enough, which is not always a single case in practice, especially for personalized medicine. On the other hand, the sample sizes of drug-induced gene expression profiles are generally large. In this study, we propose a new drug repositioning approach (HDgS), in which the drug signature is first identified from drug-induced gene expression profiles, and then connected to the gene expression profiles of disease samples to find the potential drugs for patients. In order to take the dependencies among genes into account, the human protein complexes (HPC) are used to define the drug signature. The proposed HDgS is applied to the drug-induced gene expression profiles in LINCS and several types of cancer samples. The results indicate that the HPC-based drug signature can effectively find drug candidates for patients and that the proposed HDgS can be applied for personalized medicine with even one patient sample.**

***Index Terms*—Drug repositioning, drug signature, human protein complex, personalized medicine.**

I. Introduction

IN TRADITIONAL pharmaceutical industry, putting a new drug in the market is very costly and time-consuming, about ten years and 1 billion US dollars are common in development [1], [2]. Nevertheless, the related budgets are still expanding rapidly. In traditional drug discovery pipeline, four major procedures are essential: drug discovery, pre-clinical, clinical trials and regulatory approval [3]. Several thousands of small compound candidates are typically studied to develop one new drug. However, in many projects, there's no drug that can be taken to the market successfully.

In recent decades, drug repositioning has identified some novel treatments for existing drugs, such as sildenafil, thalidomide, zidovudine, minoxidil, celecoxib, *etc* [4]. Sildenafil is the most well-known compound in drug repositioning. It was developed for the treatment of coronary artery disease in the 1980s [5], and repurposed to the treatment of erectile dysfunction in the 1990s [6]. Thalidomide was used as a sedative and is now being used to treat multiple myeloma [7].

Two types of approaches have been proposed for drug repositioning initially, which are phenotypic screening and target-based approaches [8]. In the first decade of 21st century, 45 small compounds were proposed by those approaches, 28 of which were identified by phenotypic screening [9], [10]. However, both two types of approaches have some limitations. In phenotypic drug screening, small animal models and cell-based models are necessary. The robustness and relevance of models influence the success of screening [11]. In target-based methods, researchers indicated that only 435 effective drug targets had been proposed [12].

Recently, many high-throughput platforms have been developed to measure the expression of genes, and a number of biological databases have been constructed. Many computational approaches have been proposed to use the data more efficiently and identify drug candidates, which are pathway-based methods [13], [14], similarity-based methods [15], [16], network-based methods [17]–[20], signature-based methods [1], [21]–[24], *etc*. The computational approaches are able to handle a large number of drug profiles and identify potential drugs for the specific disease in a short period [25].

Lamb *et al.* constructed Connectivity Map (CMap) database which consists of 6,100 profiles under different drug cultures and cell lines [26], [27]. Three main components were utilized in their research. A drug perturbation profile was utilized to describe the differential expression of a drug. A gene signature was a group of significantly expressed genes to represent a disease. A matching strategy was used to connect the drug perturbation profile and the gene signature for producing a connection score [28]. A negative score meant an inversion among them. The drug candidates were identified according to their connection scores.

Manuscript received October 31, 2020; revised July 29, 2021; accepted August 30, 2021. Date of publication October 19, 2021; date of current version November 5, 2021. This work was supported in part by the Natural Science and Engineering Research Council of Canada (NSERC), China Scholarship Council (CSC) and in part by the National Natural Science Foundation of China under Grants U19A2064 and 61428209. *(Corresponding author: Fang-Xiang Wu.)*

Fei Wang and Yulian Ding are with the Division of Biomedical Engineering, University of Saskatchewan, Saskatoon, Saskatchewan S7N 5A9, Canada (e-mail: few266@mail.usask.ca; yud146@mail.usask.ca).

Xiujuan Lei is with the School of Computer Science, Shaanxi Normal University, Xi'an 710119, China (e-mail: xjlei@snnu.edu.cn).

Bo Liao is with the School of Mathematics and Statistics, Hainan Normal University, Haikou 571158, China (e-mail: dragonbw@163.com).

Fang-Xiang Wu is with the Division of Biomedical Engineering, Department of Mechanical Engineering and Department of Computer Science, University of Saskatchewan, Saskatoon, Saskatchewan S7N 5A9, Canada (e-mail: faw341@mail.usask.ca).

Digital Object Identifier 10.1109/JBHI.2021.3120933

However, a few number of cell lines and small compounds were contained in CMap database. Among those small compounds, the Food and Drug Administration (FDA)-approved drugs, whose safeties had been studied, were even fewer. Phase I of the Library of Integrated Network-Based Cellular Signatures (LINCS) program was published in 2015, and the sample size of drug perturbation profiles was increased from 6,100 in CMap to 1.3 million [29].

Based on CMap and LINCS databases, many signature-based approaches have been proposed to identify candidates for drug repositioning [30]–[33]. In the databases, the expression profiles are based on gene features. In those approaches, a signature is a group of genes that are selected independently. Actually, there are some interactions among genes, in the developments of diseases [34]–[38]. In order to reflect the dependencies of genes, the associations between gene-gene interactions, protein-protein interactions and diseases have been studied [39], [40]. A protein complex is a group of proteins that have strong interactions with each other [41]. The properties of protein complexes and their relationships with diseases have been studied in many studies [42]–[44]. Wang *et al.* utilize the human protein complexes (HPCs) to identify new signatures from cancer samples and predict drug candidates for them [1].

In the existing signature-based approaches, a signature is identified from disease samples and compared with the drug perturbation profiles in CMap or LINCS database. In either statistical or network-based approaches, a large number of disease samples are critical in identifying signatures. However, when the disease set has a few samples, it's difficult to identify a reliable signature. These approaches can't especially handle samples from only a few patients.

In this study, instead of creating an HPC-based disease signature from patient samples, we propose an HPC-based drug signature (HDgS) approach to identify drug signatures and predict drug candidates. Based on the HPC information, all drug perturbation profiles and disease samples are transformed into the type of HPCs. An HPC-based drug signature is identified from all the HPC profiles of a specific drug. For disease samples, a differential expression profile of a patient is generated. The connection score between an HPC-based drug signature and a patient profile is calculated. Finally, each patient has a list of drugs. After counting the frequencies of drugs that appeared in all lists, ten drugs with the largest frequencies are identified as drug candidates. In the experiments, we compare HDgS with the HPC-based disease signature approach and three other types of drug signatures. Our HDgS approach achieves the highest prediction rates in four types of cancers. The proposed approach can even be used to identify drugs for a single patient, and known drugs are among the prediction results. At the end of the experiments, the annotations, treatments, and literature evidences of the drug candidates are discussed.

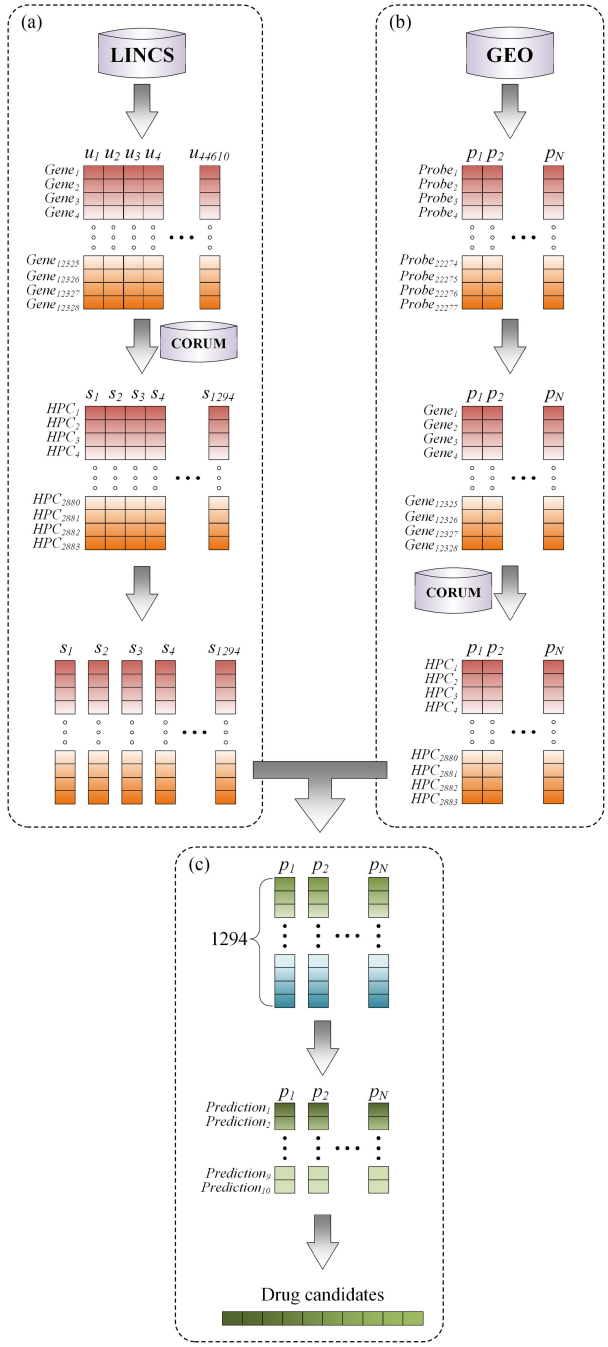

Fig. 1. The flowchart of our HPC-based drug signature approach. (a) Producing an HPC signature for each drug. (b) Transforming patient gene expression profiles to HPC profiles. (c) Matching drug HPC signatures to the patient HPC profiles, and producing a list of candidate drugs. *p* represents a patient and *N* is the number of patients, *u* is a drug profile and *s* is a merged profile for each drug. The number of approved drugs in LINCS is 1,294.

II. Materials and Methods

In this section, we discuss the datasets used in our HDgS approach and the procedures to generate the drug candidates, as shown in Fig. 1. The human protein complex information in the comprehensive resource of mammalian protein complexes (CORUM) database [45] are utilized in Fig. 1(a) and Fig. 1(b) to provide the mapping between genes and protein complexes. The drug perturbation profiles in LINCS are used to produce the

drug signatures, which are matched with the patient profiles to generate a list of drug candidates.

A. Design of Study

The basic idea in our study is to generate a negative connection between a drug signature and a patient profile of a specific disease. The negative connection indicates an opposite effect between a drug and a disease represented by gene expression profiles, which may reflect a potential treatment for the drug to the disease. In Fig. 1(a), we apply HPC information to describe the drug signatures. In Fig. 1(b), the patient profiles are transformed from the form of genes to the form of HPCs. A matrix of connection scores is calculated, as shown in Fig. 1(c). In each patient of a specific disease, the top predictions are generated and merged to produce a list of candidate drugs for the given disease. Our proposed method has been implemented in MatLab, and the codes are available at https://github.com/flykingwf for users.

B. Datasets and Pre-Processing

Three types of data are utilized in our HDgS approach, including the drug perturbation data, patient sample data, and the HPC data.

The HPC data is downloaded from the comprehensive resource of mammalian protein complex (CORUM) database [46], which contains 4,273 protein complexes, out of which 2,916 are HPCs. All HPCs cover 4,274 genes. In order to connect with other types of data, those 4,274 genes must match with Entrez gene IDs. After matching, 2,916 HPCs and 3,092 genes remain. Since some HPCs don't encompass any genes that can be matched, as shown in Fig. 2(a), we focus on the complexes that contain at least one matched gene. As a result, 2,883 HPCs are used to be the basic features in this study.

The drug perturbation profiles are downloaded from the LINCS database [29]. Phase I of LINCS database is published in the Gene Expression Omnibus (GEO) database [47]. The expression values of only 978 genes have been measured in LINCS, where these 978 genes are "landmark gene," while the other genes are "inferred genes". The values of inferred genes are calculated based on the values of landmark genes.

These 978 landmark genes are sufficient to recovery 82% information in CMap, where 22,277 gene expression values per profile are measured. In LINCS, there are 12,328 genes in a total of landmark genes and inferred genes, and 1,319,138 profiles produced from 42,080 perturbations and 72 cell lines.

In LINCS database, the types of perturbations are small molecule drugs, shRNAs, cDNAs, and biologics. Since drug repositioning is to find some novel treatment for existing drugs, whose safeties have been studied. In this study, we focus on the drugs that have been approved by FDA and DrugBank [48]. As a result, 1,294 drugs are used in this study. The histogram of the drugs and profiles are shown in Fig 2(b). The numbers of profiles vary over drugs, while many drugs have a larger number of profiles. In a previous study [1], we have generated the maps between HPCs and LINCS genes. Here drug perturbation profiles are transformed from the type of genes to HPCs, and the value of an HPC is a combination of the gene values in the HPC.

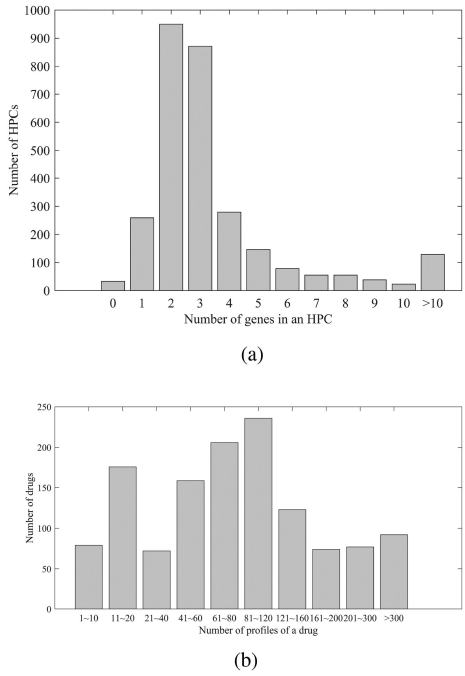

Fig. 2. The statistic of drugs and HPCs in the dataset. (a) The distribution of the number of HPCs vs. the number of genes per HPC. (b) The distribution of the number of drugs vs. the number of profiles per drug in LINCS.

TABLE I
INFORMATION OF DATASETS

Cancers	Datasets	Platforms	Disease sample sizes
Lung Cancer	GSE10072	GPL96	32
	-Stage 1		15
	-Stage 2		9
	-Stage 3		6
	-Stage 4		2
	GSE19804	GPL570	59
	-Stage 1		35
	-Stage 2		12
	-Stage 3		12
	GSE27262-Stage 1	GPL570	25
Breast Cancer	GSE10780	GPL570	42
	GSE15852	GPL96	43
	GSE50948	GPL570	40
Colorectal Cancer	GSE21510	GPL570	40
	GSE41258	GPL96	43
	GSE49355	GPL96	12
Prostate Cancer	GSE46602	GPL570	14
	GSE69223	GPL570	15

Stage 1, 2, 3 and 4 are four stages of lung cancer in the datasets.

The patient samples are downloaded from the GEO database [47]. In this study, 11 datasets of four common cancers are obtained, as shown in Table I. Among them, two platforms are referred to produce gene expression profiles. One is GPL96, where 22,283 probe sets are utilized to measure gene expression values. Another one is GPL570, where 54,675 probe sets are included. The three datasets of lung cancer come from four different stages. So the lung cancer profiles are divided into four subsets, each representing a cancer stage. In order to analyze data

from different platforms, the first step is to select the common probe sets between them, which are 22,777 in CMap. Then the probe sets are transformed into the type of LINCS genes. Since some probe sets may refer to the same gene, the gene expression value is the average of the probe sets which are referred to the same gene. The next mapping step is the same as those LINCS profiles to get the HPC profiles. The cancer datasets from different platforms are transformed into the same type of HPCs. After comparing the tumor tissue samples to the normal tissue samples, a differential HPC profile is generated.

C. HPC-Based Drug Signature Procedures

In this section, we present the procedures to identify our HPC-based drug signature from LINCS database. The profiles are generated from the LINCS Level 5 data, which consists of the differential expressions of the drug perturbations in different concentrations, durations, and cell lines.

In order to reflect the dependencies of genes, HPC is used as the component of signature instead of individual genes in this study. As shown in Fig. 2(a), many complexes contain at least two genes. In our previous study of HPC-based disease signature [1], we chose the average value of the genes in the complex to be the value of the complex. However, the importance of the genes in a complex may not be equal. In this study, we use the Pearson Correlation Coefficient (PCC) to calculate the weights of genes. Additionally, we calculate another type of weight from the Spearman Correlation Coefficient (SCC). We also compare the approach of PCC weights with that of average weights and SCC weights in Section III.

The fingerprinting vector of a gene consists of differential expression values across all profiles. A correlation matrix for a complex is constructed by pair-wise fingerprinting vectors among all genes in the same complex. Then the weight of a gene in the complex is the average correlation to all other genes. All the weights are normalized and summed to 1. The differential expression value of a complex is the linear combination of the gene differential expression values with their weights.

The original drug perturbation profiles are in the form of genes. After mapping genes to HPCs by the weight approach, the novel profiles are in the form of HPCs. If an HPC has a value larger than 1, it is treated as an up-regulated HPC in the profile, while if it has a value smaller than -1, it is a down-regulated HPC. Among all the profiles of a drug, the HPC, which is either up-regulated or down-regulated in at least half of profiles, is labeled as either an up-regulated HPC or a down-regulated HPC of the drug, respectively. Each HPC has a differential frequency among the profiles, and the up- and down-regulated HPCs are sorted together in descending order according to their frequencies. The length of HPC-based drug signature is determined in Section III.

D. Matching Procedure

After generating HPC-based drug signatures and patient differential HPC profiles, the next procedure is matching them together and calculating the matching scores. The matching method is the same which we used with disease signatures [1], [32].

Before matching, a rank list $PR = \{pr_1, pr_2, \ldots, pr_H\}$ is proposed to replace the patient differential HPC profile $PV = \{pv_1, pv_2, \ldots, pv_H\}$, where pv_i is the value of HPC_i, pr_i is its rank in the list and *H* is 2,883. The HPCs are sorted in ascending order according to their values in *PV*, where $min(PR) = 1$ and $max(PR) = H$.

Meanwhile, the signature is divided into two parts, one is the list of down-regulated HPCs, and the other one contains up-regulated HPCs. $score_{up}$ and $score_{down}$ are calculated as follows:

$$score_{up} = \sum_{i=1}^{H_{up}} (H + 1 - pr_{upi}). \tag{1}$$

$$score_{down} = -\sum_{j=1}^{H_{down}} (H + 1 - pr_{downj}). \tag{2}$$

where H_{up} is the length of the up-regulated list while H_{down} is that of the down-regulated list. up_i is the i^{th} HPC in the up-regulated list while $down_j$ is the j^{th} HPC in the down-regulated list.

A possible maximum score of the connection is calculated as follows:

$$poss = \sum_{i=1}^{M} (H + 1 - i). \tag{3}$$

where *M* is the length of signature. Finally, a connection score between an HPC-based drug signature and a patient profile is calculated as follows:

$$score_H = \frac{score_{up} + score_{down}}{poss}. \tag{4}$$

The possible range of $score_H$ is [-1,1], where a negative score reflects an inversion of the connection, which means that the drug may reverse the disease condition and have a potential treatment for it.

In our experiments, we use Matlab to implement our algorithm. Its computational time complexity is O(*MN*), while *M* is the number of drugs and *N* is the number of patients. The code can be downloaded on https://github.com/flykingwf.

E. Evaluation Metrics

In previous sections, we have produced a ranked drug list for a patient. The drugs are sorted in ascending order according to their connection scores. The top ten drugs are formed a new list for the following prediction. Therefore, we have *N* lists for a specific disease, while *N* is the number of patients. The frequency of each drug that appears on all lists is summarized. Drugs are sorted in descending order according to their frequencies. The ten most frequent drugs are selected as the drug candidates. Their uses as potential treatments for the diseases and literature evidences are discussed in Section III.

In the experiments, the competing methods also produce ten drug candidates. Among the drug candidates, some drugs have been studied about their treatments for the specific disease.

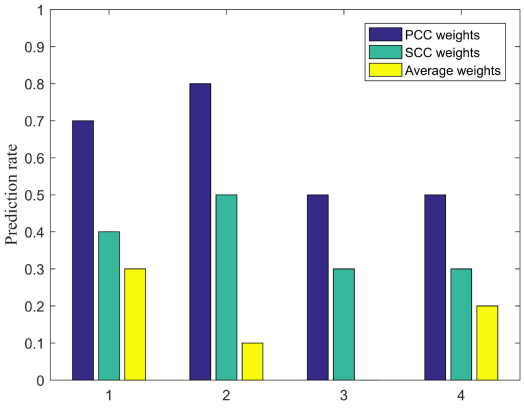

Fig. 3. The prediction rates between three types of weighting approaches.

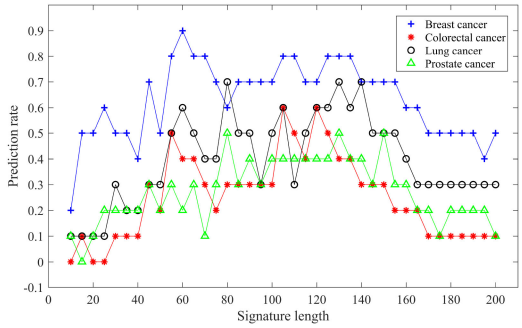

Fig. 4. The plot of the prediction rate vs. the length of signature.

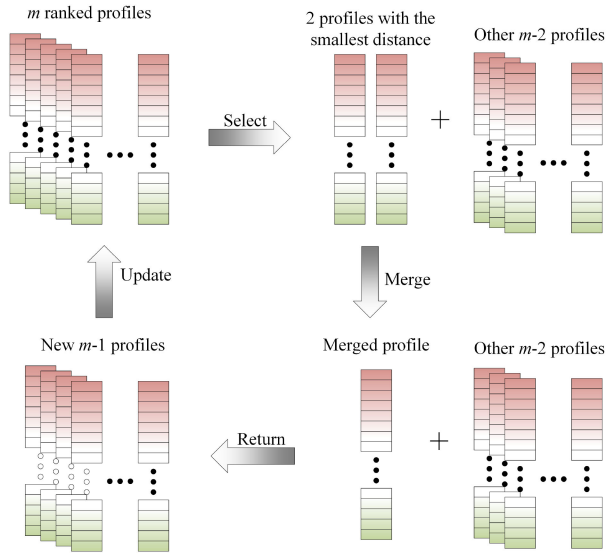

Fig. 5. The iteration steps when identifying a PRL from the profiles of a drug.

Therefore, we use "known drugs" to describe them. The other drugs in the results may have potential treatments for the disease, and we call them "potential drugs". The prediction rate is the rate of known drugs in the results. In the experiments, we use prediction rates to compare various methods.

III. Experiments and Results

As reported by the World Health Organization (WHO) in 2018, lung, breast, colorectal, and prostate cancers are the four most common cancers in the world [49]. Therefore, in this study, we apply our HPC-based drug signature approach to the four cancers and compared it with other approaches.

In Section II-C, we have discussed the PCC weights in calculating HPC values from gene values. To ensure the advantage of PCC weights in HPC-based drug signatures, we first compare them with the SCC weights and average weights, as shown in Fig. 3. The signatures via PCC weights achieve higher prediction rates than the other two types of weights. One possible reason is that genes within an HPC are not equal, while by averaging their values, all genes are treated equally. In SCC, the ranks may weaken the influence of the most differentially expressed genes. In the PCC weighting procedure, the correlations are different, a few genes may have negative correlations with other genes in the HPC. The weighting procedure is the way to enhance the genes with high positive correlations. The length of signature is another parameter that affects the prediction results. Fig. 4 shows the prediction rates over various signature lengths from 10 to 200 with an increase of 5 for four diseases. From Fig. 4, the best rate is achieved at the different signature lengths for the different diseases. In this study, we only present the results with its best signature length for a specific disease.

In the previous study [1], we propose an HPC-based disease signature approach. In this study, we apply those two HPC-based signatures to identify drug candidates for four common cancers. Additionally, we utilize three different types of drug signatures in the experiments. The first type is the drug Prototype Ranked List (PRL) signature [50], [51], where the profiles of the same drug are merged together hierarchically, as shown in Fig. 5. A set D is used to reflect a given drug with M ranked profiles. Then the Spearman's Footrule distance is calculated between each pair of them. The two profiles with the smallest distance are deleted from the set D and summed together arithmetically. The new ranked profile is generated and added to the set D. The iteration repeats until there's only one profile in the set. The gene signature contains the same number of top and bottom 50 genes.

The second type is DrugSig, which is an online drug signature resource proposed by Wu *et al* [52]. 5,913 drug signatures of 1,295 drugs are downloaded from the resource. Each signature contains 500 up-regulated genes and 500 down-regulated genes. The most different aspect is that there's no rank among the drug signature, which means all genes have the same weight. Similarly, genes in disease signatures don't have any ranks. The matching score is the rate of overlap:

$$score_{DrugSig} = \frac{up_{overlap} + down_{overlap}}{length\ of\ the\ disease\ signature}. \quad (5)$$

where the $up_{overlap}$ is the number of common genes between the disease up-regulated gene list and the drug down-regulated gene list, the $down_{overlap}$ is the number of common genes between the disease down-regulated gene list and the drug up-regulated

TABLE II
PREDICTION RATES OF THE FIVE APPROACHES

Cancers	HDgS	HPC-based disease	PRL	DrugSig	Landmark
Lung	**0.7**	0.6	0.3	0.4	0.6
-Stage 1	**0.7**	0.3	0.2	0.4	**0.7**
-Stage 2	**0.6**	0.3	0.2	0.4	0.3
-Stage 3	**0.6**	0.1	0.2	0.2	0.3
-Stage 4 - P1	**0.7**	0.0	0.3	0.2	0.2
-Stage 4 - P2	**0.7**	0.0	0.3	0.2	0.2
Breast	**0.8**	0.6	0.6	0.6	0.4
Colorectal	**0.6**	**0.6**	0.5	0.3	0.1
Prostate	**0.5**	0.4	0.4	0.4	0.3

NULL: Don't have corresponding result. P1 and P2 are two patients in the forth stage.

gene list. The matching score reflects the reverse of the two signatures.

Although several approaches have been proposed to process the LINCS profiles, some researchers prefer to identify drug signatures directly from the LINCS profiles, containing the 978 landmark genes [53]. The third type of compared signature in this study is the landmark signature. One thing that should be noted is that the profiles are not merged into a consensus one, so there may be some replicates in the prediction lists.

In the experiments, each method produces a list of ten drugs. As discussed in Section II-E, we compare the prediction rate of known drugs in the list. The prediction rate indicates the confidence that other drug candidates have the potential for the same treatment. Additionally, we collect the number of publications on PubMed, associated with the candidate drugs for specific cancer.

The prediction rates of five approaches in four types of cancers are listed in Table II. In all four cases, our HDgS approach produces the highest prediction rates. In lung cancer stage 1 and colorectal cancer, there's 1 more approach that can achieve the same prediction rates with HDgS. In the experiment of a single patient, our proposed HDgS approach can achieve a prediction rate of 0.7, the same as in the whole dataset.

Besides the prediction rate, the frequency rate of a given drug is used to reflect the portion of patients for whom the drug has been identified as a drug candidate. The drug candidates for four cancers and their frequency rates are listed in Tables III–VI. The treatments and annotations of drugs are discussed in the following sections.

A. Lung Cancer

In 2.09 million cases of lung cancers [49], about 85% are non-small cell lung cancer (NSCLC), while the others are small cell lung cancer (SCLC). As shown in Table III, ten small compounds are identified by the whole patient group, seven of which are known drugs. Additionally, seven different drugs are identified by the five subsets of patients.

Triptolide is a diterpenoid epoxide that is produced from the Tripterygium Wilfordii plant. It can decrease cell migration and invasion of lung cancer in vitro [54]. Maraviroc is an antiretroviral drug. It reduces lung tumor growth via decreasing the migration of C–C chemokine receptor type 5 (CCR5)+ regulatory T cells [55]. Palbociclib is an inhibitor of the cyclin-dependent kinases 4 (CDK4) and CDK6. The combination treatment of palbociclib and selumetinib is effective in the models of NSCLC [56].

Crizotinib is an anaplastic lymphoma kinase (ALK) inhibitor that has shown treatments for NSCLC. It is superior to standard chemotherapy in advanced NSCLC patients with ALK rearrangement [57]. Neratinib is a tyrosine kinase inhibitor (TKI) anticancer drug. It has promising activity in NSCLC, according to both preclinical and human studies [58]. Oxytetracycline is a broad-spectrum antibiotic. It displays apparent inhibitions on the proliferation of A549 lung cancer cells [59]. Caffeine is a central nervous system (CNS) stimulant [60]. It increases apoptosis of lung cancer, which is killed by cisplatin, through the inhibition of ataxia telangiectasia mutated- and Rad3-related (ATR) activation [61].

Ciglitazone is a thiazolidinedione. It inhibits growth and induces apoptosis of NSCLC cells through decreased expression of phosphoinositide-dependent protein kinase 1 (PDK1) [62]. Fenretinide is a synthetic retinoid derivative. It induces apoptosis of SCLC cells and inhibits its growth [63]. Geldanamycin is a 1,4-benzoquinone ansamycin antitumor antibiotic. The association of Ad-mda7 gene and geldanamycin inhibits lung cancer cell motility and induces cell death [64].

Seven drugs are predicted to have potential treatments for lung cancer, two of which have been studied for the treatment for tumors and cancers. Lomerizine has the clinical potential to reverse tumor multidrug resistance [65]. GSK-1059615 is a type of kinase inhibitor and has been used in trials studying the treatment for solid tumors and breast cancer [66]. About the other five predictions, more information about the associations with cancers needs to be studied in the future. Terconazole is an antifungal drug. Guanadrel is an antihypertensive agent. Lofexidine is a non-opioid prescription medicine used to treat high blood pressure. Tinidazole is a drug for protozoan infections. Oxetacaine is a potent local anesthetic.

B. Breast Cancer

Breast cancer is the most common cancer (2.09 million cases) in women [49]. As shown in Table IV, ten small compounds are predicted by our proposed HPC-based drug signature, nine of which are known drugs.

Palbociclib is a medication for breast cancer that has been sold in the market [67], [68]. Etoposide is a medication for several types of cancers. It is an active and well-tolerated regimen in metastatic breast cancer (MBC) patients [69]. Tretinoin is a medication for leukemia. The tretinoin-loaded lipid core nanocapsules reduce the breast cancer cell viability even at lower concentrations [71]. Teniposide is a chemotherapeutic medication used in the treatment of childhood acute lymphocytic leukemia and several cancers. It suppresses the growth of breast tumor in vivo [72].

Tunicamycin is a mixture of homologous nucleoside antibiotics. The combination of trastuzumab and tunicamycin shows effective treatments for HER2-positive breast cancer cells [73].

TABLE III
DRUGS PREDICTED FOR LUNG CANCER

Labels	Names	The frequency rates in the groups of patients						Num of Ref.
		Whole dataset	Stage 1	Stage 2	Stage 3	Stage 4-P1	Stage 4-P2	
Known drugs	Triptolide	0.948	0.960	0.905	0.944	1	1	58
	Maraviroc	0.871	0.893	0.762	0.889	1	1	6
	Palbociclib	0.629	0.613	0.762	0.556	NULL	1	79
	Crizotinib	0.517	0.493	0.524	0.611	1	NULL	2074
	Neratinib	0.431	0.427	0.222	0.500	1	1	70
	Oxytetracycline	0.414	0.440	NULL	0.556	1	NULL	18
	Caffeine	0.336	0.387	NULL	NULL	1	NULL	143
	Ciglitazone	NULL	NULL	0.333	NULL	NULL	1	26
	Fenretinide	NULL	NULL	NULL	NULL	1	1	46
	Geldanamycin	NULL	NULL	NULL	NULL	NULL	1	64
Potential drugs	Lomerizine	0.500	0.520	0.477	0.389	1	1	0
	Terconazole	0.414	0.360	0.477	0.556	1	NULL	0
	GSK-1059615	0.371	0.373	0.333	0.444	NULL	NULL	0
	Guanadrel	NULL	NULL	0.286	0.333	NULL	NULL	0
	Lofexidine	NULL	NULL	NULL	NULL	1	NULL	0
	Tinidazole	NULL	NULL	NULL	NULL	NULL	1	3
	Oxetacaine	NULL	NULL	NULL	NULL	NULL	1	0

NULL: The drug is not on the prediction list of the corresponding group of patients. Num of Ref.: The number of publications associated with the predicted drug for lung cancer on PubMed.

TABLE IV
DRUGS PREDICTED FOR BREAST CANCER

Labels	Names	Frequency rates	Num of Ref.
Known drugs	Palbociclib	0.824	784
	Etoposide	0.560	1195
	Tretinoin	0.432	657
	Teniposide	0.408	39
	Tunicamycin	0.280	95
	Triptolide	0.272	53
	Idarubicin	0.272	107
	Cytarabine	0.264	262
Potential drugs	PHA-793887	0.512	1
	Norethisterone	0.344	255

TABLE V
DRUGS PREDICTED FOR COLORECTAL CANCER

Labels	Names	Frequency rates	Num of Ref.
Known drugs	Isosorbide	0.863	4
	Triptolide	0.726	18
	Maraviroc	0.526	2
	Palbociclib	0.474	5
	Tivozanib	0.347	4
	Trametinib	0.263	29
Potential drugs	Lomerizine	0.884	0
	Alverine	0.589	0
	Oxetacaine	0.558	0
	Tyloxapol	0.495	0

TABLE VI
DRUGS PREDICTED FOR PROSTATE CANCER

Labels	Names	Frequency rates	Num of Ref.
Known drugs	Palbociclib	0.897	13
	Triptolide	0.690	28
	Maraviroc	0.517	3
	Cisplatin	0.310	1138
	Rucaparib	0.276	49
Potential drugs	Alverine	0.897	0
	Brompheniramine	0.552	1
	Tyloxapol	0.414	0
	Disopyramide	0.379	1
	PHA-793887	0.276	0

Triptolide has shown antitumor effects for lung cancer and predicted in Section III. It inhibits the viability of breast cancer cells and significantly reduces the tumor weight and volume [74]. Idarubicin is an antineoplastic that has shown treatments against breast cancer [75], [76]. Cytarabine is a chemotherapy medication used to treat leukemia. Some cases have suggested that treatment of intrathecal liposomal cytarabine in patients with leptomeningeal metastasis of breast cancer is feasible [77].

In this study, PHA-793887 and norethisterone are predicted to be potential drugs for breast cancer. PHA-793887 is a CDK4 inhibitor, while the CDK4/6 inhibitors could sensitize a sub-type of breast cancer to PI3K inhibitors [78]. Norethisterone is a synthetic progestational hormone. It is a very weak inhibitor of CYP2C9 and CYP3A4, which are expressed in breast cancer tissues [79]. Studies about CYP3A4 indicate that it may play a role in breast carcinogenesis [80]. Further studies may concentrate on how to enhance its inhibitions on those genes.

C. Colorectal Cancer

Colorectal cancer is the third most common cancer (1.80 million cases) in the world [49]. ten small compounds are predicted in the results, as shown in Table V, six out of which are known drugs.

Isosorbide is a bicyclic chemical compound. The combination of aspirin and isosorbide mononitrate shows synergistic apoptosis-inducing effects in human colon cancer cells [81]. Triptolide has been identified in Sections III-A and III-B. It also induces apoptosis of human colon cancer cells and inhibits proliferation [82]. Maraviroc has been used in the treatment of breast cancer. It induces significant apoptotic effects in colorectal cancer cells [83]. Palbociclib has been discussed in Sections III-A and III-B. It promotes colon cancer cell death and induces apoptosis [84].

Tivozanib is a type of kinase inhibitor, and the inhibition is helpful in the treatment of colorectal cancer [85]. In a phase II study, the combination of tivozanib and everolimus shows treatment in 50% of the patients with metastatic colorectal cancer [85]. Trametinib is a MEK inhibitor drug with anti-cancer activities. The combination of dabrafenib and trametinib shows treatment for patients with metastatic colorectal cancer [86], [87].

Four drugs are predicted to have potential treatment for colorectal cancer, two of which have been studied the connections with cancers. Lomerizine is predicted to be a potential drug for both lung cancer and colorectal cancer, that it has the clinical potential to reverse tumor multidrug resistance [65]. Alverine is a medication for gastrointestinal disorders. The combination of MG132 and it shows cytotoxic effects on breast cancer cells [88]. Oxetacaine is a potent local anesthetic. Tyloxapol is a surfactant.

D. Prostate Cancer

Prostate cancer is the second common cancer (1.28 million cases) in men. As shown in Table VI, ten small compound are predicted, five of which are known drugs.

Palbociclib and triptolide are identified in all four cancers. Palbociclib is a novel medication for prostate cancer. A phase II study shows that it may help slow the growth of prostate cancer [89]. Triptolide induces prostate cancer cell death [90]. Maraviroc has been identified in lung and prostate cancers. It reduces prostate tumor bone metastasis in immunocompetent mice [91]. Cisplatin is a chemotherapy medication used to treat a number of cancers, including prostate cancer [92], [93]. Rucaparib is a poly ADP ribose polymerase (PARP) inhibitor, which is used as an anti-cancer medication. It has antitumor activities in prostate cancer patients [94].

Alverine and tyloxapol are predicted to be potential drugs for both colorectal and prostate cancers. Brompheniramine is a histamine H1 antagonist, that histamine has some interactions with cell proliferation and tumor growth [95]. PHA-793887 is a CDK inhibitor, which is used to treat cancers by preventing overproliferation of cancer cells [96]. Disopyramide is an antiarrhythmic medication.

E. Discussion

In the experiments, we have studied our proposed framework in four types of cancers, including lung cancer, breast cancer, colorectal cancer, and prostate cancer. Among the predicted drug lists for each cancer, some known drugs have been either utilized in the treatment of cancer or studied *in vitro* and *vivo* trials. The lowest rate of the known drugs in the list is 50% in prostate cancer, while even 80% of drugs in the candidate list for breast cancer have shown treatments in previous studies. Those results indicate that our HDgS approach can be used to predict drug candidates for cancers. In this study, we have adopted the HPC-based drug signatures to connect with patient profiles. The datasets used in this study contain only one type of cancer in each sample. However, in principle, if a sample is from a patient with comorbidity, the potential drugs for such a patient should be different from those patients with a single disease. If there are some datasets from patients with comorbidity available, we would like to apply our proposed method to them in the future.

IV. Conclusion

In this study, we have proposed a novel HPC-based drug signature (HDgS) for drug repositioning. The HPCs are utilized to describe dependencies between genes. Comprehensive experiments have been conducted to evaluate the performance of HDgS and other approaches. In the experiments, each patient is given a list of drug candidates, and the predictions for the cancer are according to the frequency analysis of the lists. The proposed HDgS can identify known drugs for most of the patients. The prediction rates of HDgS are larger than those of the competing approaches. When dealing with two patient samples separately, the proposed HDgS approach can identify seven known drugs, most of which are the same as those from the whole dataset. Based on literature evidences, many of the potential drugs also have anti-cancer properties.

References

[1] F. Wang *et al.*, "Human protein complex signatures for drug repositioning," in *Proc. 10th ACM Int. Conf. Bioinf., Comput. Biol. Health Informat.*, Niagara Falls, NY, USA, 2019, pp. 42–50.

[2] F. Emmert-Streib *et al.*, "The human disease network: Opportunities for classification, diagnosis, and prediction of disorders and disease genes," *Syst. Biomed.*, vol. 1, no. 1, pp. 20–28, Jan. 2013.

[3] H. Matthews, J. Hanison, and N. Nirmalan, "Omics'-informed drug and biomarker discovery: Opportunities, challenges and future perspectives," *Proteomes*, vol. 4, no. 3, pp. 1–12, Sep. 2016.

[4] S. Pushpakom *et al.*, "Drug repurposing: Progress, challenges and recommendations," *Nature Rev. Drug Discov.*, vol. 18, no. 1, pp. 41–58, Jan. 2019.

[5] J. S. Shim and J. Liu, "Recent advances in drug repositioning for the discovery of new anticancer drugs," *Int. J. Biol. Sci.*, vol. 10, no. 7, pp. 654–663, 2014.

[6] M. Boolell *et al.*, "Sildenafil: An orally active type 5 cyclic GMP-specific phosphodiesterase inhibitor for the treatment of penile erectile dysfunction," *Int. J. Impotence Res.*, vol. 8, no. 2, pp. 47–52, Jun. 1996.

[7] T. T. Ashburn and K. B. Thor, "Drug repositioning: Identifying and developing new uses for existing drugs," *Nature Rev. Drug Discov.*, vol. 3, no. 8, pp. 673–683, Aug. 2004.

[8] G. Jin and S. Wong, "Toward better drug repositioning: Prioritizing and integrating existing methods into efficient pipelines," *Drug Discov. Today*, vol. 19, no. 5, pp. 637–644, May 2014.

[9] D. C. Swinney and J. Anthony, "How were new medicines discovered?," *Nature Rev. Drug Discov.*, vol. 10, no. 7, pp. 507–519, Jul. 2011.

[10] M. R. Hurle *et al.*, "Computational drug repositioning: From data to therapeutics," *Clin. Pharmacol. Therapeutics*, vol. 93, no. 4, pp. 335–341, Apr. 2013.

[11] M. Szabo *et al.*, "Cell and small animal models for phenotypic drug discovery," Drug Design, *Develop. Ther.*, vol. 11, pp. 1957–1967, Jun. 2017.

[12] M. Rask-Andersen, M. S. Almén, and H. B. Schiöth, "Trends in the exploitation of novel drug targets," *Nature Rev. Drug Discov.*, vol. 10, no. 8, pp. 579–590, Aug. 2011.

[13] S. K. Tan *et al.*, "Drug repositioning in glioblastoma: A pathway perspective," *Front. Pharmacol.*, vol. 9, pp. 1–19, Mar. 2018.

[14] H. Zhao *et al.*, "Novel modeling of cancer cell signaling pathways enables systematic drug repositioning for distinct breast cancer metastases," *Cancer Res.*, vol. 73, no. 20, pp. 6149–6163, Oct. 2013.

[15] P. Xuan *et al.*, "Drug repositioning through integration of prior knowledge and projections of drugs and diseases," *Bioinformatics*, vol. 35, no. 20, pp. 4108–4119, Oct. 2019.

[16] C. K. Yan *et al.*, "BiRWDDA: A novel drug repositioning method based on multisimilarity fusion," *J. Comput. Biol.*, vol. 26, no. 11, pp. 1230–1242, Nov. 2019.

[17] X. Zeng *et al.*, "Target identification among known drugs by deep learning from heterogeneous networks," *Chem. Sci.*, vol. 11, no. 7, pp. 1775–1797, Jan. 2020.

[18] Y. H. Feng *et al.*, "DPDDI: A deep predictor for drug-drug interactions," *Chem. Sci.*, vol. 21, no. 1, pp. 1–15, Dec. 2020.

[19] C. C. Yang and M. Zhao, "Mining heterogeneous network for drug repositioning using phenotypic information extracted from social media and pharmaceutical databases," *Artif. Intell. Med.*, vol. 96, pp. 80–92, May 2019.

[20] X. Zhou *et al.*, "*In silico* drug repositioning based on drug-miRNA associations," *Brief. Bioinf.*, vol. 21, no. 2, pp. 498–510, Mar. 2020.

[21] H. Haeberle *et al.*, "Identification of cell surface targets through meta-analysis of microarray data," *Neoplasia*, vol. 14, no. 7, pp. 666–669, Jul. 2012.

[22] P. Sanseau *et al.*, "Use of genome-wide association studies for drug repositioning," *Nature Biotechnol.*, vol. 30, no. 4, pp. 317–320, Apr. 2012.

[23] P. G. O'Reilly *et al.*, "QUADrATiC: Scalable gene expression connectivity mapping for repurposing FDA-approved therapeutics," *BMC Bioinf.*, vol. 17, no. 1, pp. 1–15, Dec. 2016.

[24] F. Wang, Y. Ding, X. Lei, B. Liao, and F. Wu, "Identifying gene signatures for cancer drug repositioning based on sample clustering," *IEEE/ACM Trans. Comput. Biol. Bioinf.*, Aug. 2020, doi: 10.1109/TCBB.2020.3019781.

[25] F. Wang, X. Lei and F. X. Wu, "A review of drug repositioning based chemical-induced cell line expression data," *Curr. Med. Chem.*, vol. 27, no. 32, pp. 5340–5350, Sep. 2020.

[26] J. Lamb *et al.*, "The connectivity map: Using gene-expression signatures to connect small molecules, genes, and disease," *Science*, vol. 313, no. 5795, pp. 1929–1935, Sep. 2006.

[27] J. Lamb, "The connectivity map: A new tool for biomedical research," *Nature Rev. Cancer*, vol. 7, no. 1, pp. 54–60, Jan. 2007.

[28] M. Hollander, D. A. Wolfe, and E. Chicken, "The two-sample dispersion problem and other two-sample problems," in *Nonparametric Statistical Methods*. New York, NY, USA: Wiley, 2013, pp. 151–201.

[29] A. Subramanian *et al.*, "A next generation connectivity map: L1000 platform and the first 1,000,000 profiles," *Cell*, vol. 171, no. 6, pp. 1437–1452, Nov. 2017.

[30] S. D. Zhang *et al.*, "A simple and robust method for connecting small-molecule drugs using gene-expression signatures," *BMC Bioinf.*, vol. 9, no. 1, pp. 1–10, Dec. 2008.

[31] S. D. Zhang *et al.*, "sscMap: An extensible Java application for connecting small-molecule drugs using gene-expression signatures," *BMC Bioinf.*, vol. 10, no. 1, pp. 1–4, Dec. 2009.

[32] Q. Wen *et al.*, "Connectivity mapping using a combined gene signature from multiple colorectal cancer datasets identified candidate drugs including existing chemotherapies," *BMC Syst. Biol.*, vol. 9, no. 5, pp. 1–11, Dec. 2015.

[33] R. Shukla *et al.*, "Signature-based approaches for informed drug repurposing: Targeting CNS disorders," *Neuropsychopharmacol.*, vol. 46, no. 1, pp. 116–130, Jan. 2021.

[34] D. M. Sabatini *et al.*, "mTOR and cancer: Insights into a complex relationship," *Nature Rev. Cancer*, vol. 6, no. 9, pp. 729–734, Sep. 2006.

[35] J. Fu *et al.*, "The TWIST/Mi2/NuRD protein complex and its essential role in cancer metastasis," *Cell Res.*, vol. 21, no. 2, pp. 275–289, Feb. 2011.

[36] M. Leiserson *et al.*, "Pan-cancer network analysis identifies combinations of rare somatic mutations across pathways and protein complexes," *Nature Genet.*, vol. 47, no. 2, pp. 106–114, Feb. 2015.

[37] X. Li *et al.*, "Validation of the Hsp70-Bag3 protein-protein interaction as a potential therapeutic target in cancer," *Mol. Cancer Therapeutics*, vol. 14, no. 3, pp. 642–648, Mar. 2015.

[38] C. Wu, J. Zhu, and X. Zhang, "Integrating gene expression and protein-protein interaction network to prioritize cancer-associated genes," *BMC Bioinf.*, vol. 13, no. 1, pp. 1–10, Dec. 2012.

[39] A. Ivanov, F. Khuri, and H. Fu, "Targeting protein-protein interactions as an anticancer strategy," *Trends Pharmacological Sci.*, vol. 34, no. 7, pp. 393–400, Jul. 2013.

[40] S. van Dam *et al.*, "Gene co-expression analysis for functional classification and gene-disease predictions," *Brief. Bioinf.*, vol. 19, no. 4, pp. 575–592, Jul. 2018.

[41] V. Spirin and L. A. Mirny, "Protein complexes and functional modules in molecular networks," *Proc. Nat. Acad. Sci.*, vol. 100, no. 21, pp. 12123–12128, Oct. 2003.

[42] M. Li *et al.*, "Identifying dynamic protein complexes based on gene expression profiles and PPI networks," *BioMed Res. Int.*, vol. 2014, pp. 1–10, May 2014.

[43] X. Lei *et al.*, "iOPTICS-GSO for identifying protein complexes from dynamic PPI networks," *BMC Med. Genomic.*, vol. 10, no. 5, pp. 55–66, Dec. 2017.

[44] Q. Xiao *et al.*, "A novel core-attachment-based method to identify dynamic protein complexes based on gene expression profiles and PPI networks," *Proteomics*, vol. 19, no. 5, pp. 1–7, Mar. 2019, Art. no. 1800129.

[45] A. Ruepp *et al.*, "CORUM: The comprehensive resource of mammalian protein complexes," *Nucleic Acids Res.*, vol. 36, no. suppl_1, pp. D646–D650, Oct. 2007.

[46] M. Giurgiu *et al.*, "CORUM: The comprehensive resource of mammalian protein complexes-2019," *Nucleic Acids Res.*, vol. 47, no. D1, pp. D559–D563, Jan. 2019.

[47] T. Barrett *et al.*, "NCBI GEO: Archive for functional genomics data sets-update," *Nucleic Acids Res.*, vol. 41, no. D1, pp. D991–D995, Nov. 2012.

[48] D. S. Wishart *et al.*, "DrugBank: A comprehensive resource for in *silico* drug discovery and exploration," *Nucleic Acids Res.*, vol. 34, no. suppl_1, pp. D668–D672, Jan. 2006.

[49] F. Bray *et al.*, "Global cancer statistics 2018: GLOBOCAN estimates of incidence and mortality worldwide for 36 cancers in 185 countries," *CA: A Cancer J. Clinicians*, vol. 68, no. 6, pp. 394–424, Nov. 2018.

[50] F. Iorio *et al.*, "Discovery of drug mode of action and drug repositioning from transcriptional responses," *Proc. Nat. Acad. Sci.*, vol. 107, no. 33, pp. 14621–14626, Aug. 2010.

[51] F. Iorio *et al.*, "A semi-supervised approach for refining transcriptional signatures of drug response and repositioning predictions," *PLoS One*, vol. 10, no. 10, pp. 1–21, Oct. 2015, Art. no. e0 139446.

[52] H. Wu *et al.*, "DrugSig: A resource for computational drug repositioning utilizing gene expression signatures," *PLoS One*, vol. 12, no. 5, pp. 1–11, May 2017, Art. no. e0 177743.

[53] I. W. Kim *et al.*, "Computational drug repositioning for gastric cancer using reversal gene expression profiles," *Sci. Rep.*, vol. 9, no. 1, pp. 1–10, Feb. 2019.

[54] T. A. Reno, J. Y. Kim, and D. J. Raz, "Triptolide inhibits lung cancer cell migration, invasion, and metastasis," *Ann. Thoracic Surg.*, vol. 100, no. 5, pp. 1817–1825, Nov. 2015.

[55] E. C. Halvorsen *et al.*, "Maraviroc decreases CCL8-mediated migration of CCR5$^+$ regulatory T cells and reduces metastatic tumor growth in the lungs," *Oncoimmunol.*, vol. 5, no. 6, pp. 1–15, Jun. 2016, Art. no. e 1150398.

[56] J. Zhou *et al.*, "Palbociclib, A selective CDK4/6 inhibitor, enhances the effect of selumetinib in RAS-driven non-small cell lung cancer," *Cancer Lett.*, vol. 408, pp. 130–137, Nov. 2017.

[57] A. T. Shaw *et al.*, "Crizotinib versus chemotherapy in advanced *ALK*-positive lung cancer," *New England J. Med.*, vol. 368, no. 25, pp. 2385–2394, Jun. 2013.

[58] P. Bose and H. Ozer, "Neratinib: An oral, irreversible dual EGFR/HER2 inhibitor for breast and non-small cell lung cancer," *Expert Opin. Investigational Drugs*, vol. 18, no. 11, pp. 1735–1751, Nov. 2009.

[59] J. Shao and G. Feng, "Selective killing effect of oxytetracycline, propafenone and metamizole on A549 or Hela cells," *Chin. J. Cancer Res.*, vol. 25, no. 6, pp. 662–670, Dec. 2013.

[60] A. Nehlig, J. L. Daval, and G. Debry, "Caffeine and the central nervous system: Mechanisms of action, biochemical, metabolic and psychostimulant effects," *Brain Res. Rev.*, vol. 17, no. 2, pp. 139–170, May 1992.

[61] G. Wang, V. Bhoopalan, D. Wang, L. Wang, and X. Xu, "The effect of caffeine on cisplatin-induced apoptosis of lung cancer cells," *Exp. Hematol. Oncol.*, vol. 4, no. 1, pp. 1–9, Dec. 2015.

[62] S. Hann *et al.*, "Repression of phosphoinositide-dependent protein kinase 1 expression by ciglitazone via Egr-1 represents a new approach for inhibition of lung cancer cell growth," *Mol. Cancer*, vol. 13, no. 1, pp. 1–13, Dec. 2014.

[63] G. P. Kalemkerian, R. Slusher, S. Ramalingam, S. Gadgeel, and M. Mabry, "Growth inhibition and induction of apoptosis by fenretinide in small-cell lung cancer cell lines," *JNCI: J. Nat. Cancer Inst.*, vol. 87, no. 22, pp. 1674–1680, Nov. 1995.

[64] A. Pataer *et al.*, "Enhancement of adenoviral MDA-7-mediated cell killing in human lung cancer cells by geldanamycin and its 17-allyl-amino-17-demethoxy analogue," *Cancer Gene Ther.*, vol. 14, no. 1, pp. 12–18, Jan. 2007.

[65] N. Shiraki *et al.*, "Increase in doxorubicin cytotoxicity by inhibition of P-glycoprotein activity with lomerizine," *Biol. Pharmaceut. Bull.*, vol. 24, no. 5, pp. 555–557, May 2001.

[66] GSK-1059615, DrugBank, Jun. 2020. [Online]. Available: https://go.drugbank.com/drugs/DB11962

[67] F. Serra *et al.*, "Palbociclib in metastatic breast cancer: current evidence and real-life data," *Drugs Context*, vol. 8, pp. 1–16, Jul. 2019.

[68] B. O'Leary *et al.*, "Early circulating tumor DNA dynamics and clonal selection with palbociclib and fulvestrant for breast cancer," *Nature Commun.*, vol. 9, no. 1, pp. 1–10, Mar. 2018.

[69] X. H. Yang *et al.*, "Reconstitution of caspase 3 sensitizes MCF-7 breast cancer cells to doxorubicin-and etoposide-induced apoptosis," *Cancer Res.*, vol. 61, no. 1, pp. 348–354, Jan. 2001.

[70] D. G. Cheung, "Action of CDK inhibitor PHA-848125 in ER-negative breast cancer with MicroRNA-221/222 overexpression," Ph.D. dissertation, Ohio State Univ., Columbus, OH, USA, 2017.

[71] E. Schultze *et al.*, "Tretinoin-loaded lipid-core nanocapsules overcome the triple-negative breast cancer cell resistance to tretinoin and show synergistic effect on cytotoxicity induced by doxorubicin and 5-fluororacil," *Biomed. Pharmacother.*, vol. 96, pp. 404–409, Dec. 2017.

[72] B. Chu *et al.*, "Preparation and evaluation of teniposide-loaded polymeric micelles for breast cancer therapy," *Int. J. Pharmaceutics*, vol. 513, no. 1-2, pp. 118–129, Nov. 2016.
[73] X. Han *et al.*, "Tunicamycin enhances the antitumor activity of trastuzumab on breast cancer *in vitro* and *in vivo*," *Oncotarget*, vol. 6, no. 36, pp. 38912–38925, Nov. 2015, Art. no. 38912.
[74] H. Li *et al.*, "Triptolide inhibits human breast cancer MCF-7 cell growth via downregulation of the ERα-mediated signaling pathway," *Acta Pharmacologica Sinica*, vol. 36, no. 5, pp. 606–613, May 2015.
[75] Idarubicin, DrugBank, Oct. 2021. [Online]. Available: https://go.drugbank.com/drugs/DB01177
[76] U. Gunduz *et al.*, "Idarubicin-loaded folic acid conjugated magnetic nanoparticles as a targetable drug delivery system for breast cancer," *Biomed. Pharmacother.*, vol. 68, no. 6, pp. 729–736, Jul. 2014.
[77] E. Laakmann, I. Witzel, and V. Müller, "Efficacy of liposomal cytarabine in the treatment of leptomeningeal metastasis of breast cancer," *Breast Care*, vol. 12, no. 3, pp. 165–167, Jun. 2017.
[78] S. R. Vora *et al.*, "CDK 4/6 inhibitors sensitize PIK3CA mutant breast cancer to PI3K inhibitors," *Cancer Cell*, vol. 26, no. 1, pp. 136–149, Jul. 2014.
[79] R. Schmidt *et al.*, "CYP3A4, CYP2C9, and CYP2B6 expression and ifosfamide turnover in breast cancer tissue microsomes," *Brit. J. Cancer*, vol. 90, no. 4, pp. 911–916, Feb. 2004.
[80] C. Keshava, E. C. McCanlies and A. Weston, "CYP3A4 polymorphisms-Potential risk factors for breast and prostate cancer: A HuGE review," *Amer. J. Epidemiol.*, vol. 160, no. 9, pp. 825–841, Nov. 2004.
[81] X. Wang *et al.*, "Synergistic apoptosis-inducing effect of aspirin and isosorbide mononitrate on human colon cancer cells," *Mol. Med. Rep.*, vol. 12, no. 3, pp. 4750–4758, Sep. 2015.
[82] L. Zhao *et al.*, "Effect of triptolide on human colorectal cancer HCT116 cell proliferation, autophagy and apoptosis," *Chin. Pharmacological Bull.*, vol. 32, no. 10, pp. 1399–1403, Jan. 2016.
[83] A. Pervaiz, S. Ansari, M. R. Berger, and H. Adwan, "CCR5 blockage by maraviroc induces cytotoxic and apoptotic effects in colorectal cancer cells," *Med. Oncol.*, vol. 32, no. 5, pp. 1–10, May 2015.
[84] J. Zhang, L. Zhou, S. Zhao, D. T. Dicker, and W. S. El-Deiry, "The CDK4/6 inhibitor palbociclib synergizes with irinotecan to promote colorectal cancer cell death under hypoxia," *Cell Cycle*, vol. 16, no. 12, pp. 1193–1200, Jun. 2017.
[85] B. M. Wolpin *et al.*, "Multicenter phase II study of tivozanib (AV-951) and everolimus (RAD001) for patients with refractory, metastatic colorectal cancer," *Oncologist*, vol. 18, no. 4, pp. 377–378, Apr. 2013.
[86] R. B. Corcoran *et al.*, "Combined BRAF and MEK inhibition with dabrafenib and trametinib in BRAF V600-mutant colorectal cancer," *J. Clin. Oncol.*, vol. 33, no. 34, pp. 4023–4031, Dec. 2015.
[87] E. Bangi *et al.*, "A personalized platform identifies trametinib plus zoledronate for a patient with KRAS-mutant metastatic colorectal cancer," *Sci. Adv.*, vol. 5, no. 5, pp. 1–11, May 2019, Art. no. eaav 6528.
[88] D. Ju, X. Wang, and Y. Xie, "Dyclonine and alverine citrate enhance the cytotoxic effects of proteasome inhibitor MG132 on breast cancer cells," *Int. J. Mol. Med.*, vol. 23, no. 2, pp. 205–209, Feb. 2009.
[89] Palbociclib in Patients With Metastatic Castration-Resistant Prostate Cancer, U.S. National Institutes of Health, National Library of Medicine, Jul. 2021. [Online]. Available: https://clinicaltrials.gov/ct2/show/NCT02905318
[90] W. Huang *et al.*, "Triptolide inhibits the proliferation of prostate cancer cells and down-regulates SUMO-specific protease 1 expression," *PLoS One*, vol. 7, no. 5, pp. 1–17, May 2012, Art. no. e 37693.
[91] D. Sicoli *et al.*, "CCR5 receptor antagonists block metastasis to bone of v-Src oncogene-transformed metastatic prostate cancer cell lines," *Cancer Res.*, vol. 74, no. 23, pp. 7103–7114, Dec. 2014.
[92] T. Nomura, M. Yamasaki, Y. Nomura, and H. Mimata, "Expression of the inhibitors of apoptosis proteins in cisplatin-resistant prostate cancer cells," *Oncol. Rep.*, vol. 14, no. 4, pp. 993–997, Oct. 2005.
[93] S. Dhar, F. X. Gu, R. Langer, O. C. Farokhzad, and S. J. Lippard, "Targeted delivery of cisplatin to prostate cancer cells by aptamer functionalized Pt (IV) prodrug-PLGA-PEG nanoparticles," *Proc. Nat. Acad. Sci.*, vol. 105, no. 45, pp. 17356–17361, Nov. 2008.
[94] W. Abida *et al.*, "Rucaparib in men with metastatic castration-resistant prostate cancer harboring a BRCA1 or BRCA2 gene alteration," *J. Clin. Oncol.*, vol. 38, no. 32, pp. 3763–3772, Nov. 2020, doi: 10.1200/JCO.20.01035.
[95] B. Blaya *et al.*, "Histamine and histamine receptor antagonists in cancer biology," *Inflamm Allergy Drug Targets*, vol. 9, no. 3, pp. 146–157, Jul. 2010.
[96] M. E. Law, P. E. Corsino, S. Narayan, and B. K. Law, "Cyclin-dependent kinase inhibitors as anticancer therapeutics," *Mol. Pharmacol.*, vol. 88, no. 5, pp. 846–852, Nov. 2015.